Invited Paper
(Proc. SPIE Vol. 5246, pp. 333-344; ITCom Conference 2003)

Limits of DWDM with gratings and Fabry-Perots & alternate solutions

C. Roychoudhuri, D. Lee and Y. Jiang; Photonics Lab., Physics Department, University of Connecticut

(Contact: Chandra@phys.uconn.edu)

and

S. Kittaka, M. Nara, V. Serikov and M. Oikawa; Nippon Sheet Glass Co., Ltd.

(Contact: ShigeoKittaka@mail.nsg.co.jp)

ABSTRACT

High resolution DWDM devices based on the principles of gratings (planar, Bragg, AWG, etc.) and Fabry-Perots (etalon, Lummer-Gehrke plate, etc.) suffer from inherent limitations due to (i) temporal pulse stretching of data, and (ii) broadening of time integrated spectral (demuxed) fringes. While the relation, $d\nu_F dt > 1$, can account for these limitations, our analysis imply that $d\nu_F$ does not represent real, physical frequencies. We explain the broader implications of this interpretation in designing DWDM devices based on gratings and Fabry-Perots and illustrate how to use prisms, photonic crystals and non-linear devices for very high data rate per channel.

Keywords: DWDM, spectrometry of short pulses, time diffraction

1. UNDERSTANDING GRATINGS AND FABRY-PEROTS AS PULSE REPLICATERS

Gratings and Fabry-Perots (FP) replicate an incident light beam into a train of periodically delayed N beams, where N is the number of lines (or, steps) for a grating and a few-times the finesse number for a FP. FP's, consisting of a pair of beam splitters, replicate an incident beam by amplitude division . Gratings, consisting of spatially extent and periodic delay steps, replicate the incident beam by wave front division. When the optical imaging system for an FP or a grating is arranged in such a way as to physically superpose the replicated N beams on a detector, one can record a narrow intensity fringe whose width is inversely proportional to N^2. Since light moves with a finite and fixed velocity in a homogeneous medium, and FP & gratings are linear (but with well defined boundary value differences), the light propagation must be causal in the classical sense. Consequently, a finite time pulse will be replicated into N periodically delayed pulses with partial superposition, giving rise to time-varying interference fringe patterns [1-18]. This is the foundation of our "time-varying" approach to understand and analyze time varying and time integrated, multiple beam fringe produced by gratings and FP's when illuminated by a pulsed light. The simple cases of an FP and an echelle grating are illustrated below in Fig.1.

Since, most spectra are measured at the Fraunhofer (or, far-field, or, spatial Fourier transform) plane, we simplify our computational algorithm to find the superposition effects in the spectral plane by summing the plane wave fronts at the far-field with appropriate temporal (phase) delays and pulse amplitude variation of all the diffracted wave fronts produced by each one of the N-steps of the grating. If we are observing a m-th order fringe, then the path difference between the consecutive grating steps, or one FP round trip is $\Delta = m\lambda$. Then the time delay is given by Eq.(1).

$$\tau = \Delta/c = (\Delta/\lambda)(\lambda/c) = m/\nu, \quad \text{or, } m = \nu\tau \tag{1}$$

Now, if our input signal is an arbitrarily narrow delta-pulse and the regular step delay is τ, the impulse response, h(t), is given by the summation of N delayed delta-pulses, $\delta(t-n\tau)$. If a(t) is the amplitude of a finite size input data pulse, the out put amplitude, i(t), is the summation of N time- and phase-delayed pulses, given by the Eq.(2) below.

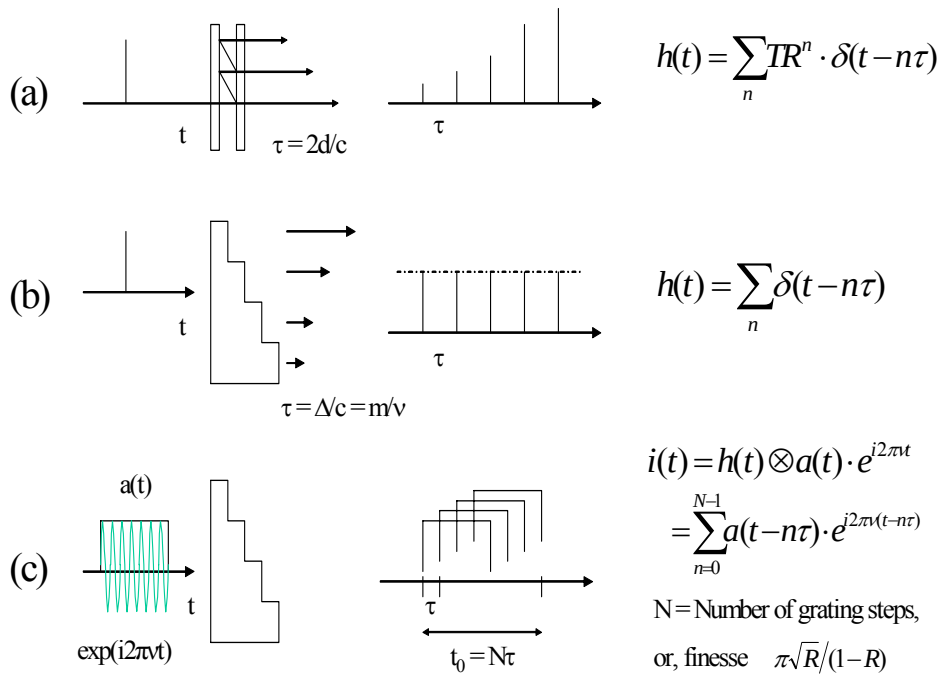

Figure 1. Temporal impulse response of gratings and Fabry-Perots and their spectrometer time constant, t_0. (a) and (b) show temporal pulse replication by a Fabry-Perot and a grating, respectively. (c) demonstrates the partial superposition of the replicated and time-delayed pulses. This leads to both temporal stretching of the output pulse and broadening of the N-beam interference fringe intensity (or, apparent spectral fringe).

$$i_p(t) = h(t) \otimes a(t) \cdot e^{i2\pi\nu_q t} = \sum_{n=0}^{N-1} \left[\frac{TR^n}{or, N} \right] a(t - n\tau) \cdot e^{i2\pi\nu_q (t-n\tau)} \qquad (2a)$$

Where generalized impulse response is, $$h(t) = \sum_{n=0}^{N-1} \left[\frac{TR^n}{or, N} \right] \delta(t - n\tau) \qquad (2b)$$

And the Fourier transform is, $$\tilde{h}(\nu) = \sum_{n=0}^{N-1} \left[\frac{TR^n}{or, N} \right] e^{i2\pi\nu(t-n\tau)} \qquad (2c)$$

Where, TR^n denotes the reduction in amplitudes in an FP due to multiple reflection and transmission [9]. For a grating, TR^n is replaced by (1/N) as the amplitude diffracted by each of the N-slit out of the total amplitude incident on the n-slit grating. Such a simple algorithm gives very accurate results for all free-space gratings (far-field) and FPs and for pulses containing 100's of oscillations of the EM field. This is true for most DWDM devices and even for 40 GBit data, the average pulses are about 10 ps and a single optical period is on the order of a few femto seconds. For AWGs and photonic crystal devices, where wave-guide properties are dominant, simple far-field conditions cannot be invoked. In such cases, accurate results are computed by using FDTD method. Before we compute Eq.(2) and interpret the results, let us review classical spectroscopy with CW light.

2. UNDERSTANDING CLASSICAL SPECTROSCOPY

We anchor our position with well-understood CW, monochromatic light of steady unit amplitude, such that a(t) = $\exp(i2\pi\nu_q)$. The steady state but instantaneous fringe amplitude is given by Eq.3, where all the N wave fronts are simultaneously present, all the time, with periodic phase delay of $n\tau$.

$$i_{cw}(t,\nu,\tau) = \sum_{n=0}^{N-1}\left[\frac{TR^n}{or,N}\right]e^{i2\pi\nu_q(t-n\tau)} \qquad (3a)$$

Please, note that Eqns. 2c and 3 are mathematically identical. The ν in Eq.2c represents any generalized Fourier frequency from the Fourier kernel, $\exp(i2\pi\nu t)$. The ν_q in Eq.3 represents the unique carrier frequency of a CW, monochromatic light, which is the physical solution of the Maxwell's wave equation. This "semantic" difference will be important in later discussions. We identify this mathematical equivalency in Eq.3b below:

$$\left|\tilde{h}(\nu)\right|^2 \equiv \tilde{H}(\nu_F) = \left|i_{cw}(\nu_q)\right|^2 \equiv I_{cw}(\nu_q) \qquad (3b)$$

The subscripts "F "and "q" have been inserted in Eq.3 a & b to underscore that ν_F is derived from the Fourier transform kernel (mathematical frequency) and ν_q represents the actual E-vector oscillation (physical, or carrier) frequency of the EM field. The normalized, steady, instantaneous, intensity is given by the square modulus of Eq.3a [9]. As mentioned before, we are using, T = R = 1 for gratings:

$$\begin{aligned} I_{cw,\,FP}(\nu_q,\tau) &= T^2/[1+R^2-2R\cos(4\pi\nu_q\tau)] \\ &= T^2/[1+R^2-2R\cos(4\pi m)], \qquad \text{for a Fabry-Perot.} \end{aligned} \qquad (4)$$

$$\begin{aligned} \text{and,}\quad I_{cw,G}(\nu_q,\tau) &= (1/N^2)\,[\sin^2(N\pi\nu_q\tau)/\sin^2(\pi\nu_q\tau)] \\ &= (1/N^2)\,[\sin^2(N\pi m)/\sin^2(\pi m)] \\ &= \frac{1}{N}+\frac{2}{N^2}\sum_{p=1}^{N-1}(N-p)\cos(2\pi p\nu\tau), \qquad \text{for a grating.} \end{aligned} \qquad (5)$$

The last, alternate, expression for the grating fringes represents a summation of all possible two-beam interference intensities produced by the N beams from the N grating slits. This non-traditional representation brings more physics by bringing conceptual continuity between the expressions for CW and pulsed light (see Eq.17 in the next section) and between N-beam grating interference and two-beam, Michelson Fourier transform spectroscopy. In fact, insertion of N = 2 in Eq.5 gives the traditional two-beam fringes, the basis for Fourier transform spectroscopy:

$$\begin{aligned} I_{cw,\,M}(\nu,\tau) &= (1/2)[1+\cos(2\pi\nu_q\tau)] \\ &= (1/2)[1+\cos(2\pi m)], \quad \text{for a Michelson.} \end{aligned} \qquad (6)$$

The above classical equations have been re-written in terms of the order, m, of the fringes to underscore that the fringe-axes in the spatial domain (Figs. 2 & 3), displaying the spectrum, are not truly spectral axes, although the value of the frequency corresponding to a fringe can be extrapolated from the Eq.1. This point can be appreciated from the fact that (i) multiple fringes by the same frequency can be formed on the fringe-axis, but at different order locations, or (ii) all different frequencies can be piled up as one fringe (white light fringe) at the m = 0 order fringe location (white light fringes). When the incident light consists of a single carrier frequency ν_q, and the normalized spectrum, $S_{i,cw}(\nu_q) = \delta(\nu-\nu_q)$, the out put spectral fringe is given by the convolution of the CW instrumental response function, $I_{cw,\,FP}(\nu,\tau)$ or $I_{cw,\,g}(\nu,\tau)$, and the result is the instrumental broadened fringe at a location $m_q = \nu_q\tau$. The symbol, ©, represents convolution. Note that the instrument broadened fringe, limited by the effective number of interfering beams, does not represent new optical frequencies. $S_{o,cw}(\nu_q)$ represents the instrumentally broadened spectral fringe as in Eq.7 below.

$$S_{o,cw}(\nu_q) = [I_{cw,\,FP}(\nu,\tau) \text{ or } I_{cw,\,g}(\nu,\tau)] \,©\, [S_{i,cw}(\nu_q) = \delta(\nu-\nu_q)] = [I_{cw,\,FP}(\nu_q,\tau) \text{ or } I_{cw,\,g}(\nu_q,\tau)] \qquad (7)$$

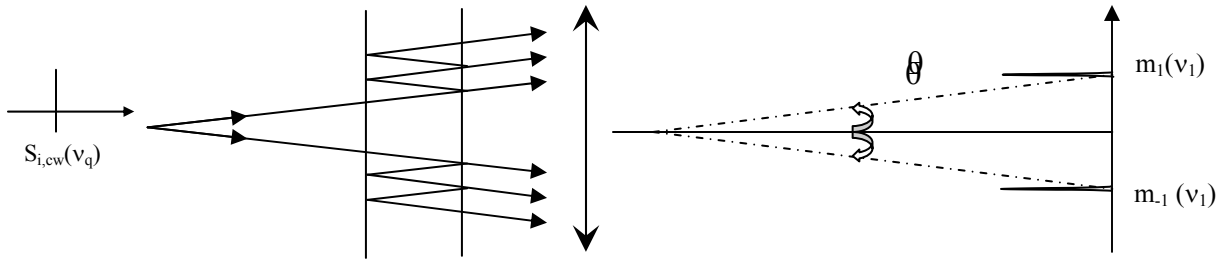

Figure 2. Schematic illustration of the location of fringe maxima and its identification with the optical carrier frequency for the case of a CW, monochromatic frequency, S(ν), passing through a Fabry-Perot interferometer.

When the incident spectrum consists of a discrete set of q monochromatic, CW, frequencies, one can observe discretely separate fringes that are formed for the same value m_q, but at separate locations, given by $m_q = \nu_q\tau$, as shown in Fig.3. This is possible because amplitudes of different optical frequencies do not interfere with (or, influence) each other by themselves [1]. Again, the widths of the individual fringes do not represent any new optical E-vector oscillations.

$$S_{o,cw}(\nu_q) = [I_{cw,\,FP}(\nu,\tau), \text{or } I_{cw,\,g}(\nu,\tau)] \copyright [S_{i,cw}(\nu_q) = \textstyle\sum_q \delta(\nu-\nu_q)] = [\textstyle\sum_q I_{cw,\,FP}(\nu_q,\tau), \text{or } \sum_q I_{cw,\,g}(\nu_q,\tau) \qquad (8)$$

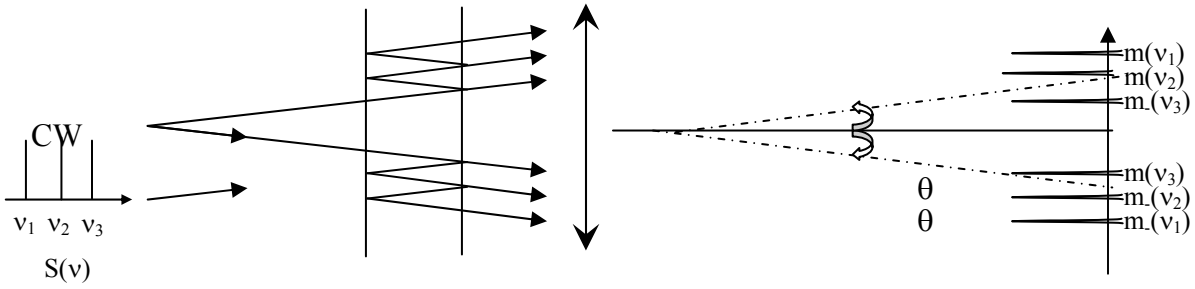

Figure 3. Representation of the "spectral" fringes due to a CW laser spectrum consisting of three narrow, longitudinal modes. Each of the spectral fringes is broadened by the CW instrumental response function given by Eq.4.

The Eqns. 7 & 8 can be summarized as:

$$S_{o,cw}(\nu) = I_{cw}(\nu) \copyright S_{i,cw}(\nu) \qquad (9)$$

where, $I_{cw}(\nu)$ is the CW instrumental response function for a grating or an FP. When the input light is a pulse, $a(t)\exp(i2\pi\nu_q t)$, the traditional approach is to take the Fourier transform of the input signal, $f(\nu - \nu_q)$, and take the normalized square modulus, $F(\nu_F - \nu_q)$, as the input spectrum.

$$a(t)\exp(i2\pi\nu_q t) \leftarrow \text{Fourier transform} \rightarrow \widetilde{f}(\nu-\nu_q) \rightarrow \text{Normalized square modulus} \rightarrow \widetilde{F}(\nu) \qquad (10)$$

Consequently, the traditional approach would imply that the out put spectral fringe due to a pulse a(t) carrying a single E-vector frequency, ν_q, is to be represented by,

$$S_{o,p}(\nu-\nu_q) = I_{cw}(\nu) \otimes \widetilde{F}(\nu-\nu_q) \equiv \widetilde{H}(\nu) \otimes \widetilde{F}(\nu) \qquad (11)$$

As we will see later, the Eq.11 does represent the quantitative value of the fringe broadening due to a pulse cut out from a single frequency, CW source, but the fringe broadening, centered at ν_q, does not represent any new carrier (or, E-vector) frequencies. The broadening is simply due to the reduction in the effective number of beams that are simultaneously present at any time out of the N replicated and delayed, superposed beams. This is already illustrated in

Fig.1 and the computational algorithm will be shown in the next section. The pulse stretching effect has to be computed from Eq.3a.

We will conclude this section by underscoring the contradictions behind the assumption that gratings or FPs can respond to the mathematical Fourier frequencies. First, Fourier decomposition integral for a time pulse is a non-causal integral and cannot represent the propagation of a causal signal of well defined velocity. Second, light beams of different frequencies do not interfere. That is, when they are physically superposed, they do not produce time pulses [1]. We have shown in this paper that simple superposition of two or more optical frequencies do not produce time varying amplitude modulation of the input CW light with a new average frequency for its E-vector. In other words, the elegant mathematics of Fourier synthesis does not represent a generalized principle of physics. Accordingly, by invoking mathematical self-consistency, one can argue that mathematical Fourier frequencies, produced by time-Fourier decomposition of a pulse, cannot represent a generalized principle of physics either. In fact, the highly successful field of Fourier transforms spectroscopy, established more than a century ago by the Nobel Laureate, Albert Michelson, is based on the hypothesis that light of different frequencies do not interfere with each other even when they are collinearly superposed. One can appreciate from the Eqns. 3 through 12, while taking the square modulus of the amplitude (photo detection process), that we always neglect the cross-terms between the amplitudes due to different optical frequencies. Detecting beat signal needs a separate discussion and is self-consistent with our approach [1].

3. TIME DOMAIN ALGORITHM FOR SPECTRAL FRINGES

Let us recall Eq.2. The time evolving, light induced signal perceived by a detector, is the square modulus of Eq.2. Very short time average required by photo detection process is achieved automatically by the mathematical operation of complex conjugate. This pulse stretching and replication are verified in references [10, 11].

$$\begin{aligned} \mathrm{I}'(t,\nu,\tau) &= \left|i_p(t)\right|^2 \\ &= \sum_{n=m=0}^{N-1} T^2R^{2n}\cdot a^2(t-n\tau) + 2\sum_{n\neq m} T^2R^{n+m}\cdot a(t-n\tau)a(t-m\tau)\cdot\cos[2\pi(m-n)\nu\tau] \end{aligned} \tag{13}$$

Time integrated fringe energy received by a detector is given by:

$$I''(\nu,\tau) = \sum_{n=m=0}^{N-1} T^2R^{2n}\cdot\int_{-T_0/2}^{+T_0/2} dt a^2(t-n\tau) + 2\sum_{n<m}^{N-1} T^2R^{n+m}\cdot\cos[(m-n)\omega_0\tau]\cdot\int_{-T_0/2}^{+T_0/2} dt a(t-n\tau)a(t-m\tau) \tag{14}$$

Where T_0 indicates the total length of the replicated pulse train. The relation is simplified by dividing the above relation throughout by the total energy of the pulse:

Then we obtain: $\int a^2(t)\,dt$

$$I'''(\nu,\tau) = \sum_{n=m=0}^{N-1} T^2R^{2n} + 2\sum_{n<m}^{N-1} T^2R^{n+m}\cdot\cos[2\pi(m-n)\nu\tau]\cdot\gamma(p\tau) \tag{15}$$

Where, γ (pτ) is the normalized time autocorrelation of the amplitude envelope, a(t):

$$\gamma(p\tau) = \frac{\int a(t-n\tau)a(t-m\tau)\,dt}{\int a^2(t)\,dt} \quad , \qquad \text{where, p = (m-n).} \tag{16}$$

For a Grating, we insert T = R = 1 and divide both sides by N^2. Then we obtain the apparent spectral fringe width, or the direct saptio-temporal impulse response for a pulse as:

$$I_{p,g}(\nu_q,\tau) \equiv \int_{-T_0/2}^{+T_0/2} dt\left|i_p(t)\right|^2 = \frac{1}{N} + \frac{2}{N^2}\sum_{p=1}^{N-1}(N-p)\cos 2\pi p\nu_q\tau \tag{17}$$

For CW light, one can substitute $\gamma(p\tau) = 1$ and recover the Eq.5, and with further insertion of N= 2, one can recover Eq.6. This derivability of CW cases from direct time domain algorithm adds conceptual strength to Eq.17. Note that when ν_q is fixed, the fringe width variation can be recorded only by varying τ, which is the case in our spectroscopy experiments. If the source radiation contains many ν_q, then the Eq.17 has to be summed over all ν_q and their respective maxima on the fringe axis will appear at τ-values given by $\nu_q \tau_q = m$ (integers).

$$\sum_{\nu_q} I_{p,g}(\nu_q \tau) = \sum_{\nu_q} \left[\frac{1}{N} + \frac{2}{N^2} \sum_{p=1}^{N-1} (N-p) \cos 2\pi p \nu_q \tau \right] \qquad (17a)$$

4. EQUIVALENCY OF TIME DOMAIN & FOURIER CONVOLUTION APPROACHES

Our objective, in this section, is to show that the Eqns. 11 and 17 are mathematically equivalent. The quantitative measurements of the broadening of the spectral fringe intensity due to an amplitude pulse, cut out from a single frequency, CW laser, are represented equally by either of the two equations. We start with the Eq.17:

$$I_{p,G}(\nu, \tau) \equiv \int_{-\infty}^{+\infty} \left| i_p(t) \right|^2 dt = \int_{-\infty}^{+\infty} \left| \tilde{i}(\nu) \right|^2 d\nu \qquad (18)$$

The last equality comes from Parseval's theorem of energy conservation. We also know by Fourier transforming first segment of the Eq.2a, that:

$$\tilde{i}(\nu) = \tilde{h}(\nu) . \tilde{f}(\nu - \nu_q) \qquad (19)$$

Hence,
$$\left| \tilde{i}(\nu) \right|^2 = \left| \tilde{h}(\nu) \right|^2 . \left| \tilde{f}(\nu - \nu_q) \right|^2 \equiv \tilde{H}(\nu) . \tilde{F}(\nu - \nu_q) \qquad (20)$$

We are now assuming that, in stead of being a constant, ν_q is a variable as Fourier frequencies supposed to. Then, insertion of Eq.20 in Eq.18 gives the final equivalency of Eq. 11 and Eq.17:

$$I_{p,G}(\nu, \tau) = \int_{-\infty}^{+\infty} \tilde{H}(\nu_q) . \tilde{F}(\nu - \nu_q) \, d\nu_q = \tilde{H}(\nu) \otimes \tilde{F}(\nu) \qquad (21)$$

However, this mathematical equivalency hides the physics that Fourier transform frequencies do not represent new physical frequencies and creates conceptual limitations in exploring different dispersive devices.

5. TIME DOMAIN COMPUTATION OF SPECTRAL FRINGES BY PLANE WAVE SUPERPOSITION

Let us consider the case of a possible high resolution echelle grating like device consisting of the following parameters. We are choosing an echelle as its parameters closely resemble currently popular AWG devices. However, the optical system is assumed to be suitable for superposing plane waves at the spectral plane, required by the Eq. 17. We have used an input square pulse of width, $\delta t = F.t_0 = 50$ ps (Fig.4a) and 20 ps (Fig.4b), where F is an arbitrary factor that helps us compare fringe widths due to CW and pulsed light. When F = 1 or greater, the pulsed fringe widths tend to get closer to CW result. So, the factor, F, can be defined as the beam overlap factor of the N replicated pulses (see Fig.5a,b). The physical meaning of the overlap factor can be appreciated from the inserts on the top right corners of Fig.5a and b. They show the delayed superposition of the replicated pulses.

Pulse stretching, or spectrometer time constant, $t_0 = N\tau = 51.5$ ps
Pulse of width, $\delta t = F.t_0 = 50$ ps (Fig.4a) and 20 ps.
Number of echelle steps, N = 50.
Operating wavelength, $\lambda = 1550$ nm.
Operating order, m = 200; step delay, $\tau = (m/\nu) = 1.03$ ps.
Rayleigh resolving power, $R = mN = 10^4$.

Such a high resolution device is not suitable for dense WDM, unless the data rate is 10 Gbit/s or less per channel.

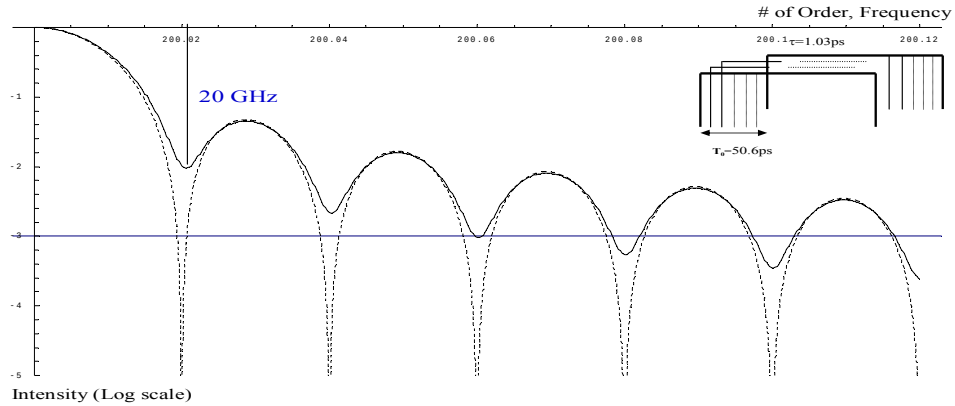

$R = mN = 10^4$ **m = 200** N = 50 | $\lambda_1 = 15500$ Å **δt = 50 ps** $\tau = 1.03$ *ps* | $\Delta\lambda_{FSR} = 77.5$ Å

Figure 4a.

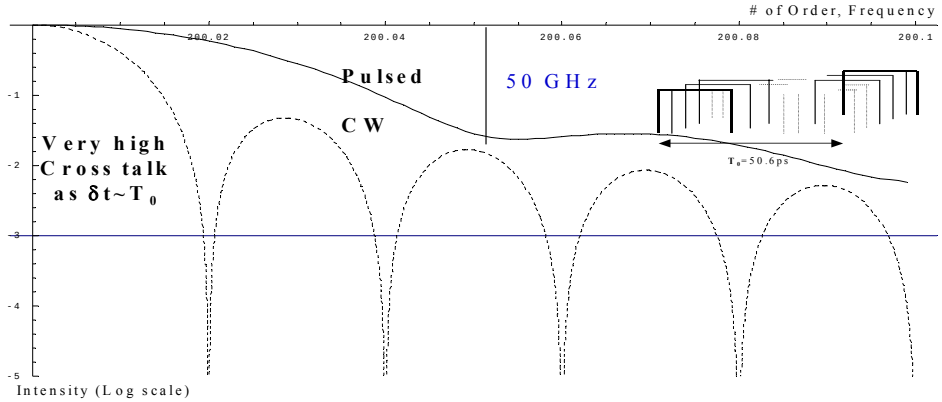

$R = mN = 10^4$ **m = 200** N = 50 | $\lambda_1 = 15500$ Å **δt = 20 ps, or** $\tau = 1.03$ *ps* | $\Delta\lambda_{FSR} = 77.5$ Å $\Delta\nu = 967.5$ GHz

Figure 4b.

Figures 4 a, b. Computation of AWG diffraction pattern for pulsed light using our algorithm (Eq.17). Comparison of the time integrated fringe energy distribution on the detector plane due to CW light (sharpest oscillatory curve represented by dots). Notice that when the pulse width tends to the pulse stretch t_0, the fringe width due to a pulse approaches the CW characteristics.

6. TIME DOMAIN COMPUTATION OF SPECTRAL FRINGES BY FDTD METHOD

For wave guide devices like AWG, plane wave superposition approach is not suitable. Actual wave fronts are to be propagated for which FDTD (finite difference time domain) method is most suitable. Accordingly, we started with the first principle (Eq. 2a or Eq.3a) and framed the problem for an AWG with the following parameters:

Pulse stretching, or spectrometer time constant, $t_0 = N\tau = 0.66$ ps
Gaussian pulses of $(1/e^2)$ intensity half-width, $\delta t = F.t_0$
Number of waveguides, N = 64.
Operating wavelength, $\lambda = 1550$ nm.
Operating order, m = 2; step delay, $\tau = (m/\nu) = 10.3$ fs.
Rayleigh resolving power, $R = mN = 128$.

The results are shown in Fig.5. The computations shown both in the section 5 (simple plane wave superposition; Fig.4) and in the section 6 (detailed wavefront propagation by FDTD; Fig.5) underscore the following. To fully exploit the capability of a grating or a Fabry-Perot like WDM device, the width of individual data pulses, $\delta t \geq t_0 = N\tau = (N\Delta/c) = Nm/\nu = R\lambda/c$, where R is the Rayleigh resolving power of the WDM device. This is equivalent to the well known "half-width" rule:

$$\delta\nu_F \, \delta t \geq 1. \qquad (22)$$

Where $\delta\nu_F$ is the half-width of the Fourier transform of the envelope function for a data pulse.

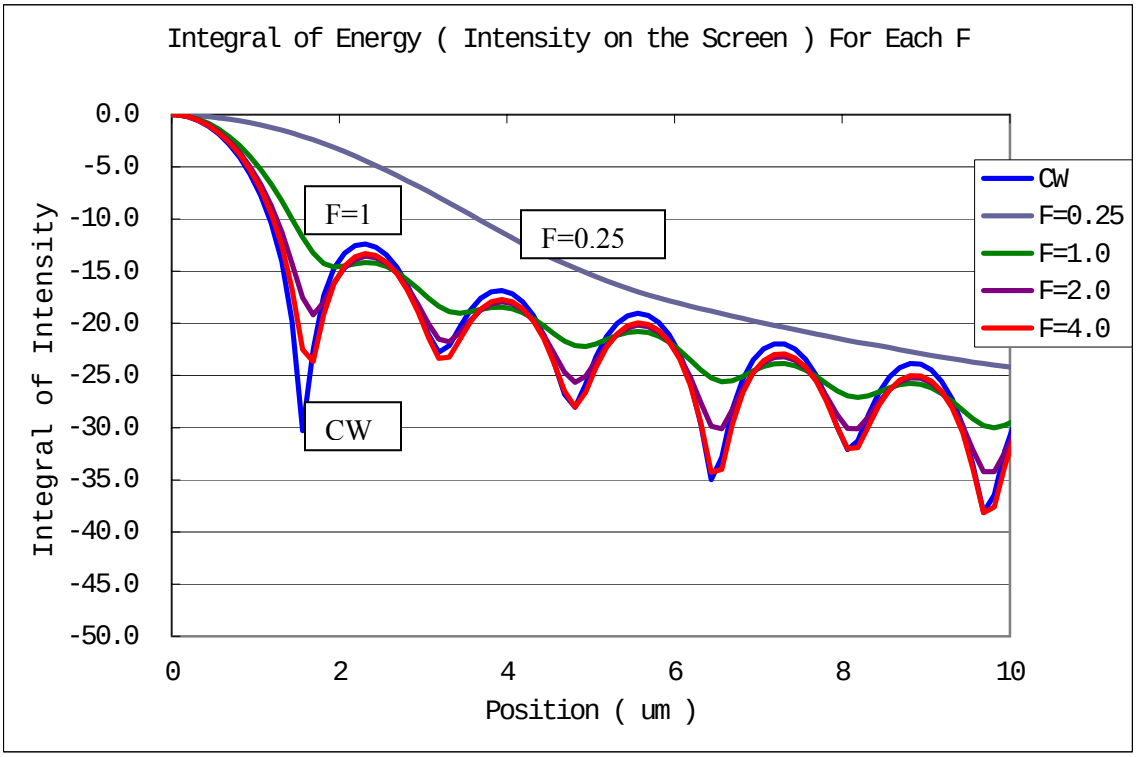

Figure 5. The plots above illustrates FDTD computation of time integrated fringe energy for various Gaussian pulses propagating through a hypothetical AWG device of 64 waveguides and of step delay m = 2. The top curve shows the case for overlapped pulses with overlap factor, F = 0.25. The next curve shows the case for overlapped pulses with overlap factor, F = 1. The very bottom curve shows the CW case. Notice that for overlap factor, F = 1 and higher, the fringes converge to the desirable CW case.

7. SUBTELTY OF DIFFRCATION FRINGES FORMED AT ZERO & HIGHER ORDERS

Let us now look at the spectral plane of a planar grating, which is the image plane of the input slit (see Fig.6). We have already developed the formulation for direct time domain computation of the fringes for m > 1. It is instructive to compare the fringe formation at m = 0 and m > 0. Let us first recapitulate the definition of resolving power, R. It is defined by Born & Wolf as the distance between the first and the last wavefront in number of wavelengths of the light.

$$R \equiv \lambda/\delta\lambda = \nu/\delta\nu = m/\delta m = Nm = \mathbf{N\Delta/\lambda} = (N\Delta/c)(c/\lambda) = N\tau\,\nu \qquad (23)$$

Let us also define the spectrometric time constant, t_0 as the total delay between the first and the last, N-th replicated pulse, which is same as the effective stretch of the out put pulse at the m-th order. It is given by,

$$t_0 \equiv N\tau = (N\Delta/c) = Nm/\nu = R\lambda/c, \qquad (24)$$

Under CW illumination (see "CW Case" in Fig.6), fringes of all orders form the same N-beam sharp fringes given by $I_{cw,G}(\nu,\tau)$ of Eq.5. However, for the "Pulse Case", the fringe at the zero order would resemble as sharp as the CW case, although the duration of the fringe will be limited to the incident pulse width δt. The fringes at locations, m > 0, are spatially broadened as per Eq.17 and temporally stretched as per Eq.24 (see also Fig.1).

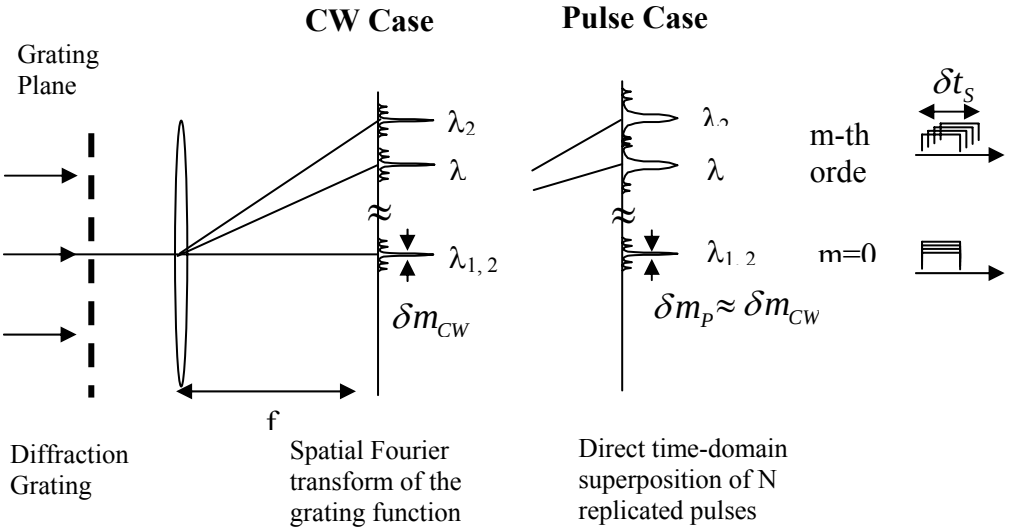

Figure 6. Diffraction fringe formation is illustrated for m=0 and a higher order for CW and short pulse illumination. At a high resolution diffraction order, the incident short pulse is stretched and the effective fringe broadened compared to that at m=0 order, due to delayed superposition of the N replicated pulses. The zero-order fringe remains sharp like the CW condition.

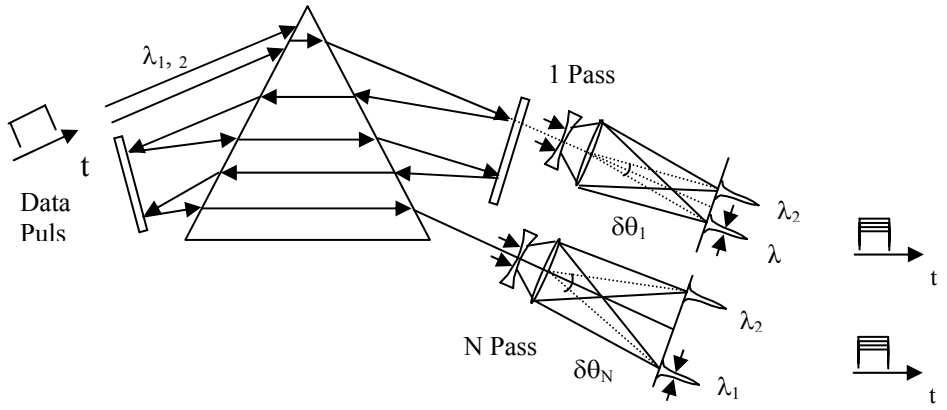

Figure 7. A short pulse as a Gaussian beam, can pass through a prism N times to produce N times higher resolution due to refraction as long as the 0-order (focused) fringe is produced as the same large f#. At this 0-order fringe, the input pulse undergoes only minor broadening due to material dispersion.

8. CLASSICAL AND PHOTONIC CRYSTAL PRISMS ALTERNATES TO GRATINGS & FP

The wavelength separating dispersive power for a grating spectrometer comes from wave front replication and their superposition with periodic delay. So, there is no dispersion at the 0-order Fraunhofer diffraction (image) location. A prism spectrometer, in contrast, forms the dispersive image at the location of the 0-order Fraunhofer diffraction. The wavelength separation originates from material dispersion, or wave front bending due to differential velocities of different wavelengths. However, the resolution of a prism spectrometer is still limited by the diffraction broadened spectral fringe, but this is a 0-order (m=0) Fraunhofer diffraction pattern. The width of this fringe is determined by the f# of the optical system. For a prism, $R= B(dn/d\lambda) \sim 10^3$ @ 1550 nm, where B is the size of the prism base [12]. We can make R N-times larger either by using N prisms, or by passing the same beam N times through the same prism. Let us target a resolving power of 1.5×10^4 (0.1 nm @1550 nm, we need 15 passes. Fig.7 depicts one mode of multiple pass along the base-apex direction. Eventually, the concept can be integrated into a planar photonic crystal wafer [14]. The broadening of a 12.5 to 8 ps pulse (40 GBit in different formats) due to material dispersion through a prism path length of 1 meter will be negligible compared to the input pulse length. The effect of differential tilt between pulse front and phase front is also negligible [15,16].

9. SECOND HARMONIC CRYSTALS AS ALTERNATES GRATINGS & FP

A wide variety of non-linear frequency conversion methods (SHG, THG, 2-photon fluorescence, etc.) can also be used to achieve dense WDM without suffering from grating-like pulse stretching effects. We are working to exploit the principle of SHG, using periodically poled Lithium-Niobate (PP-LN). Fig. 8 illustrates the principle. A chain of λ_n-resonant, PP-LN waveguides are connected by a simple optical path intercepted by a train of broad band, dichroic beam splitters (DM_n) reflecting the SHG wavelength band.

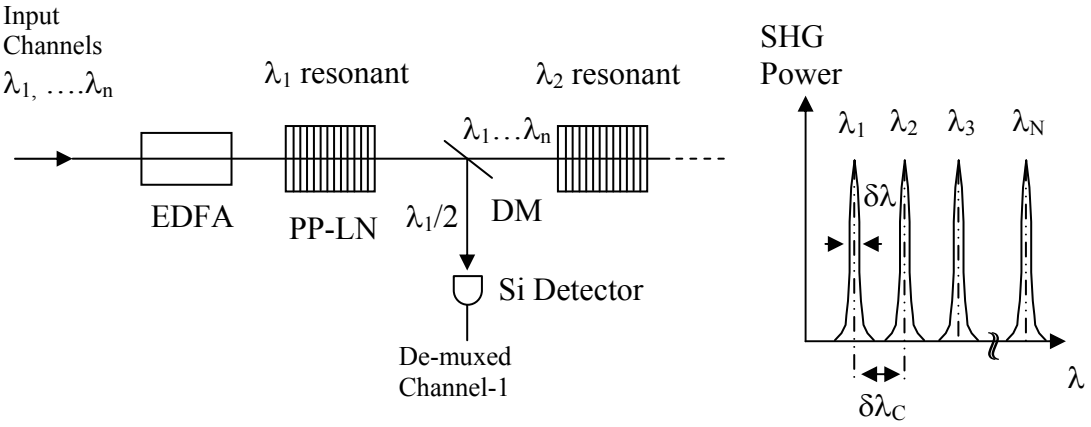

Figure 8. This sketch illustrates how SHG can effectively carry out UD-WDM with minor broadening of data pulses. Si-detector can provide system cost advantage over InP detectors by detecting 775nm instead of 1550nm.

The dense WDM wavelength set (λ_1,…λ_n), are converted to ($\lambda_1/2$,…. $\lambda_n/2$) and are separated out by the DM_n's. Besides the obvious advantage of using low cost Si-detector, this approach eliminates the need of high-resolution spectrometers like gratings and FP's. We have also significantly reduced the problem of data rate limit due to pulse stretching along with the optical resolving power limit. Pulse broadening due to material dispersion is again low. Of course, the crosstalk is now determined by the power conversion line width of the resonant PP-devices. Today's off-the-shelf PP-LN has a resonance width of $\delta\lambda_s$ = 0.2 nm with about 3 cm long crystal. Literature [13] and the manufacturers indicate that a 15 cm long waveguide will give $\delta\lambda$ = 0.1 nm @1559 nm. We see great future in integrable PP-polymeric devices.

10. WHERE DOES FOURIER MATHEMATICS REPRESENT PRINCIPLE OF PHYSICS?

Let us quickly underscore cases where Fourier transform naturally represents physics. Electric currents and potential differences are manifest only as macro electrical properties within materials (LCR circuits). Fourier synthesis is naturally manifest in these circuits. Spatial Fourier optics is the second example where Fourier transform naturally arises out of Huygens-Fresnel's (HF) principle of secondary spherical wavelets. In the far-field (or at a lens focal plane) these spherical wavelets become plane waves and HF integral simplifies into a Fourier integral (see Fig.6). This is space-space mathematical Fourier transform relation that naturally arises out of HF principle. Emergence of far-field degree of coherence due to propagation of incoherent light as the Fourier transform of the incoherent intensity function, given by van Cittert-Zernike theorem, is also a result of Huygens-Fresnel's principle [9]. The mathematical success of Fourier transform spectroscopy is based on the physical principle of non-interference of different optical frequencies and the identification of the Fourier frequency of the Fourier transform kernel with the actual optical frequency [18].

11. CONCLUSIONS

The key objective of this paper has been to underscore that for many spectrometric computations, Fourier mathematics are very powerful and useful tool. This is because both the Fourier kernel and the Maxwell's wave equation take linear superposition of sinusoidal functions. However, Fourier transformed frequencies are not one and the same as the oscillation frequency of the electric vector of a pulsed EM field emitted by atomic or molecular dipoles. Once one understands this, one can innovate many new spectrometric and WDM devices based on the principle that does not require delayed superposition of replicated pulses, as gratings and Fabry-Perots do.

ACKNOWLEDGEMENTS

It is a great pleasure for the authors of the University of Connecticut (CR, DL & YJ) to acknowledge that a part of this research has been supported by Nippon Sheet Glass Co., Ltd.

REFERENCES

1. DongIk Lee and C. Roychoudhuri "Measuring properties of superposed light beams carrying different frequencies", Optics Express, April 2003; http://www.opticsexpress.org/abstract.cfm?URI=OPEX-11-8-944.
2. C. Roychoudhuri; J. Opt. Soc. Am.; 65 (12), 1418 (1976); "Response of Fabry-Perot Interferometers to Light Pulses of Very Short Duration".
3. C. Roychoudhuri, J. Siqueiros & E. Landgrave; "Concepts of spectroscopy of pulsed light", page 87 in "Optics in Four Dimensions" Eds. M. A. Machado Gama & L. M. Narducci; American Institute of Physics, 1981.
4. C. Roychoudhuri; Am. J. Phys. 43 (12), 1054 (1975); "Demonstration Using a Fabry-Perot. I. Multiple-Slit Interference".
5. C. Roychoudhuri and T. Manzur, "Demonstration of the Evolution of Spectral Resolving Power as Superposition of Higher Order Delayed Beams", SPIE Proceedings Vol. 2525, pp.28-44 (1995); C. Roychoudhuri; Opt. Eng.; 16 (2), 173 (1976); "Passive Pulse Shaping Using Delayed Superposition".
6. C. Roychoudhuri; Opt. Eng.; 16 (2), 173 (1976); "Passive Pulse Shaping Using Delayed Superposition"
7. C. Roychoudhuri; Bol. Inst. Tonantzintla 2 (2), 101 (1976); "Is Fourier Decomposition Interpretation Applicable to Interference Spectroscopy?"
8. C. Roychoudhuri; Bulletin. Inst. Tonantzintla 2 (3), 165 (1977); "Causality and Classical Interference and Diffraction Phenomena".
9. Born and Wolf, *Principals of Optics*, Chps. 7-10, 6th edition, 1980, Cambridge University Press.
10. N. H. Schiller, "Picosecond characteristics of a spectrograph measured by a streak camera/video readout system," Opt. Comm., **35**, 451-454 (1980).
11. D.E. Leaird, A.M. Weiner, S. Kamei, M. Ishii, A. Sugita, K. Okamoto, "Generation of Flat-Topped 500GHz pulse bursts using loss engineered arrayed waveguide gratings," Photonics Tech. Lett., (2002).
12. Jenkins & White *Fundamentals of Optics*, Ch. 15, McGraw Hill.
13. L.E. Meyers, RC Eckardt, M.M. Fejert, R.L. Byer, "Quasi-phase-,matches optical parametric oscillators in bulk peridocally polled $LiNbO_3$, JOSA-B,12(n), pp-2102-2116,19995
14. V.A. Markel & T.F. George *Optics of Nano-structured Materials*, John Wiley,2001
15. S.A. Akhmanou, V.A. Vysloukh & A.S. Chirkin, "Optics of Femto-second Laser Pulses", American Institute of Physics, 1992.
16. C. Rulliere, ed., *Femto-second Laser Pulses*, Springer, 1998
17. C.X.Yu & D.T. Neilson, "Diffraction grating based (de) multiplexer using image plane transformation", IEEE JQE-8 (6), p1194, 2002.
18. Albert A. Michelson, *Studies in Optics*, University of Chicago Press, Phoenix Edition, 1968.